ASEAN Journal of Chemical Engineering 2022, Vol. 22, No. 2, 206 – 217

Effect of Al Concentration over ZnO-Al_2O_3 Physicochemical Characteristics and Removal of Remazol Red RB

Widia Purwaningrum [1,2]
Fingky Pristika Sari [1]
Julinar [1]
Adiq Ahmadi [3]
Muhammad Said [*,1,2]

[1] *Department of Chemistry, Faculty of Mathematics and Natural Sciences, Sriwijaya University, Indralaya, Sumatra Selatan, 30662, Indonesia*
[2] *Research Centre of Advanced Material and Nanocomposite, Sriwijaya University, Indralaya, Sumatra Selatan, 30662, Indonesia*
[3] *Department of Pharmacy, Faculty of Mathematics and Natural Sciences, Sriwijaya University, Indralaya, Sumatra Selatan, 30662, Indonesia*
[*]e-mail: msaidusman@unsri.ac.id

Submitted 29 October 2021 *Revised* 25 May 2022 *Accepted* 4 October 2022

Abstract. ZnO is one of the widely used semiconductors due to its high photocatalytic activity. The inactivity of ZnO in the visible range could be enhanced by combining the ZnO with Al. In this study, the photocatalytic activity of ZnO-Al_2O_3 on Remazol Red RB was investigated. The effect of the ratio mass of ZnO-Al_2O_3 (1:0.05, 1:0.07, and 1:0.10) was also evaluated. The photocatalyst would be characterized using XRD, SEM-EDX, and UV-Vis DRS. The characterization showed that photocatalysts were successfully synthesized. The XRD analysis showed that the optimum ratio mass of ZnO-Al_2O_3 was achieved by 1:0.05, with the smallest crystal size of 13.3 nm. The SEM analysis showed that the surface of ZnO-Al_2O_3 (1:0.05) was easily granulated with smaller particle sizes than ZnO, and the shape tends to clump with the composites. The EDX analysis of ZnO-Al_2O_3 confirmed the presence of Zn, O, and Al elements. The photodegradation study showed that the optimum conditions were obtained at a contact time of 180 minutes at pH 6 with 91.04% dye removal. In addition, the effect of the initial concentration of the dye was achieved at 50 ppm with a dye removal of 89.26%. The study showed that the ZnO-Al_2O_3 exhibited adequate removal of Remazol red RB.

Keywords: Composites, ZnO-Al_2O_3, Photodegradation, Photocatalyst, Remazol Red RB

INTRODUCTION

Synthetic dyes are commonly used in the industrial world due to the fact that they are not easily biodegradable in the environment (Khan et al., 2020). Different methods such as adsorption (Tejada, Villabona, and Gonzalez, 2021), coagulation (Mcyotto et al., 2021), and Advanced Oxidation Processes (AOP) (Luna-Sanguino et al., 2020) have been used in processing dye waste in order to prevent environmental pollution. The main advantage of the AOP method using photocatalysts is that organic pollutants are converted into

DOI: 10.22146/ajche.70084

CO_2, H_2O, and inorganic ions more optimally (M'Arimi et al., 2020).

ZrO_2, TiO_2, SiO_2, WO_3, and ZnO are examples of semiconductors used for the photocatalysis process (Moradipour et al., 2020). ZnO is a widely used semiconductor due to its wide band gap, low cost, great physicochemical properties, and photocatalytic activity (Elhalil et al., 2018; S. Stojadinović et al., 2015). However, the disadvantage is that it is only initiated in UV light (Stevan Stojadinović et al., 2020). In order to increase its photocatalytic activity, Combination with metals or non-metals was carried out to form composites (Cheshme khavar, Mahjoub, and Bayat Rizi, 2017). A thin layer of ZnO was combined with certain elements to improve its electrical and optical properties (Nasr et al., 2018). Furthermore, one of the promising semiconductors for enhanced photocatalytic activity is Aluminum (Al) (Luo et al., 2017). The properties of Al, such as high conductivity and low resistivity, which were achieved through composite, could hypothetically increase the photocatalytic activity of ZnO. Al also provides unique adsorption properties as well as low-cost material (Liu et al., 2015). Furthermore, it may also be used to increase the surface area of semiconductors (Munawaroh, Wahyuningsih, and Ramelan, 2017).

Remazol Red RB is one of the azo dyes which are potentially toxic and carcinogenic (Saksono, Putri, and Suminar, 2017). According to Zhang et al. (2017), nanoparticles containing 20% Al in ZnO-Al showed good degradation capacity in methyl orange, with a significant decrease in the concentration of methyl orange from 200 to 2.7 mg/L and showed as well as significant degradation thoroughly under irradiation of 30 minutes. The potential of ZnO-Al_2O_3 as a dye's removal is extensively studied and shows a remarkable due to its high adsorption ability. Tajizadegan et al. (2015) showed that the ZnO–Al_2O_3 has a high methyl orange removal efficiency compared to the single metal oxide form, which corresponds to the unique morphology of the ZnO activated as well as high surface area. Similarly, Lei et al. (2017) revealed that ZnO-Al_2O_3 provided a high adsorption capacity of up to 397 mg/g towards congo red removal, which was indicated as a highly effective dye removal. According to the literature review, the study of photodegradation on Remazol Red RB using ZnO-Al_2O_3 yet have been well studied. Therefore, this study will examine the photocatalytic activity of ZnO-Al_2O_3 towards Remazol Red RB. The effect on the mass ratio of Al to ZnO was also investigated. The photocatalyst was characterized using XRD, SEM-EDX, and UV-VIS DRS in order to see the physicochemical changes after modification was performed.

MATERIALS AND METHODS

Materials

The materials used in this study were zinc acetate dehydrate ($Zn(CH_3COO)_2{\cdot}2H_2O$, 99.5%, Merck), aluminum sulfate octadecahydrate ($Al_2(SO_4)_3{\cdot}18H_2O$, 98%, Pudak), methanol (CH_3OH, technical grade), ammonium hydroxide (NH_4OH, 28-30%, Merck), aquadest, sodium hydroxide (NaOH, 97%, Merck), hydrochloric acid (HCl, 37%, Merck), sodium chloride (NaCl, 99.5%, Merck) and Remazol Red RB dyes. Zinc acetate dehydrates, aluminum sulfate octadecahydrate, methanol, and ammonium hydroxide were used for ZnO-Al_2O_3 synthesis, while sodium hydroxide, hydrochloric acid, and sodium chloride were used for pHpzc determination.

Synthesis of ZnO

2.195 grams of $Zn(CH_3COO)_2{\cdot}2H_2O$ was dissolved in 100 mL of methanol and stirred for 2 hours. The NH_4OH solution was added dropwise until a pH of 7 was obtained. Furthermore, the resulting gel was separated and dried in an oven at 110°C for 24 hours to remove water molecules. The obtained powder was then characterized using XRD, UV-Vis DRS, and SEM-EDX (Ajala et al., 2018).

Synthesis of ZnO-Al_2O_3

The variation of mass ratio of $Zn(CH_3COO)_2{\cdot}2H_2O$ and $Al_2(SO_4)_3{\cdot}18H_2O$ are shown in Table 1.

Table 1. Mass Ratio of ZnO-Al_2O_3

Composite ZnO-Al_2O_3 ratio	$Zn(CH_3COO)_2.2H_2O$ (g)	$Al_2(SO_4)_3{\cdot}18H_2O$ (g)
1:0.05	2.195	0.333
1:0.07	2.195	0.466
1:0.10	2.195	0.66

2.195 g of $Zn(CH_3COO)_2{\cdot}2H_2O$ was dissolved in 100 mL of methanol (Solution I). An amount of $Al_2(SO_4)_3{\cdot}18H_2O$ (Table 1) was dissolved in 100 mL of methanol (Solution II). The two solutions were combined and stirred constantly for 2 hours at 70°C. Afterward, the ammonia solution was added dropwise till a pH of 7 was obtained. The resulting gel was separated and dried for 24 hours at 110°C in the oven. Last, the dried powder was calcinated in the muffle furnace for 2 hours at a temperature of 600°C. The obtained powder was then characterized using XRD, UV-Vis DRS, and SEM-EDX. In addition, the material from the best characterization results was used in the photodegradation process of Remazol Red RB.

Point of Zero Change (PHpzc) Determination

The determination of the pHpzc value was carried out with 50 mL of 0.1 M NaCl. The initial pH was adjusted from a value range of 4 to 10 by adding 0.1 M NaOH and 0.1 M HCl. Afterward, each NaCl solution that had adjusted the pH was initially added with composite ZnO-Al_2O_3 and stirred using a shaker for 24 hours before calculating the final pH of each solution.

Photodegradation Studies

The effect of time on the degradation process was carried out using a Remazol Red RB concentration with a variation of 10, 20, 30, 40, and 50 ppm along with 0.50 g of ZnO-Al_2O_3 photocatalyst. The solution was mixed with a photocatalyst and then stirred using a magnetic stirrer and subsequently irradiated using a 20 W UV lamp placed in a reactor with irradiation times of 15, 30, 45, 60, 75, and 90 minutes. The mixture was separated from the solution by centrifugation for 20 minutes at 3000 rpm. Furthermore, the degradation solution was taken, and the absorbance was measured using a UV-Vis spectrophotometer (Orion Aquamate 8000) at 531 nm.

The Remazol Red RB removal was calculated using the equation as follows: (Goudarzi & Salavati-Niasari, 2018):

$$D\ (\%) = \frac{C_o - C_t}{C_o} \times 100\% \qquad (4)$$

where:

D = Removal of Remazol Red RB (%)

C_o = Initial concentration of Remazol Red RB before degradation (ppm)

C_t = Remazol Red RB concentration after degradation at time-t (ppm)

Characterization of Photocatalyst

A Rigaku Miniflex 600 was used for X-ray diffraction analysis of the photocatalyst with

Cu Kα radiation (λ=1.54059 Å and operated at 30 kV, 10 mA). The diffraction intensity was measured as function of the diffraction angle (2θ) in 5 to 80˚ intervals, with a step width of 0.0200˚ and scan speed of 10 per minute. The morphology and surface of photocatalysts and the elemental content were observed using SEM-EDX (JEOL JSM-6510LA) with a voltage acceleration of 20kV and 3000-time magnification. The samples are coated with gold with a thickness of 48 nm. The UV-Vis DRS (Shimadzu UV–2450) with $BaSO_4$ as a reference (λ=200-800 nm) was used to identify the band gap of the photocatalyst using the Tauc Plot equation as follows: (Pradhan, Alonso, and Bizarro, 2012).

$$(\alpha\ h\ \nu) = A\ (h\nu - Eg)^{1/2} \qquad (2)$$

where:

hv = Photon energy

α = absorbance coefficient

A = absorbance

Eg = band gap energy

RESULTS AND DISCUSSIONS

Photocatalyst Characterization

The XRD characterization of ZnO and ZnO-Al_2O_3 (1:0.05), (1:0.07), and (1:0.10) are shown in Figure 1. Figure 1(a) shows the result of the diffractogram of the ZnO material. The results of the 2θ ZnO angle characterization were compared with the JCPDS card data No. 36-1451. Based on the data obtained, the characteristic angle of 2θ ZnO includes 31.77°, 34.42°, 36.25°, 47.53°, and 56.50° with plane indexes of (100), (002), (101), (102), and (110), respectively (Sangeeta et al., 2017). The resulting ZnO showed similarity with a slight shift of the peaks at an angle of 2θ when compared to the JCPDS card No. 36-1451. The shift was between 31.76°, 34.45°, 36.23°, 47.54°, and 56.58°. Subsequently, Figure 1 shows that the composite of ZnO-Al_2O_3 (1:0.05) had a typical peak at 2θ of 21.32°, 24.81°; 30.94°; which revealed identical peaks of ZnO (31°, 34°, and 36°) compared to other composites.

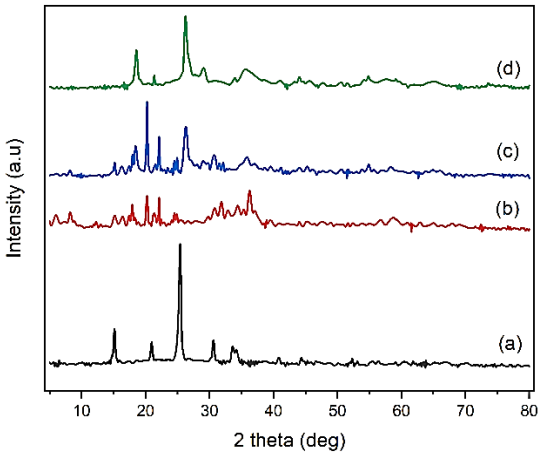

Fig. 1: The diffractogram of (a) ZnO (b) ZnO-Al_2O_3 (1:0.05) (c) ZnO-Al_2O_3 (1:0.07) and (d) ZnO-Al_2O_3 (1:0.10)

According to Murali et al. (2017) Al_2O_3 diffraction pattern generally appears at an angle 2θ of 25° to 81° with a characteristic diffraction peak of about 25°. Figure 1 revealed that the semiconductors, namely ZnO-Al_2O_3 (1:0.05), (1:0.07), and (1:0.10), showed the presence of peaks at an angle of about 31° to 36° from ZnO-Al_2O_3. This angle shifts as the Al concentration increases in the ZnO-Al_2O_3 semiconductor. The diffractogram pattern also tends to weaken with the addition of an increase in the percent concentration of Al. This is in accordance with Sa-nguanprang et al. (2019), which state that adding an Al semiconductor resulted in a wider peak in the diffractogram and a slight shift. This indicates that the crystal size and lattice parameters of ZnO were reduced. Furthermore, the smaller crystal size correlated to the larger surface area crystal, which increases the photocatalytic properties of the composite. Along with the increase in

the active surface area of the catalyst material, the contact area between the catalyst particles and pollutants also increased. This resulted in a more effective pollutant decomposition process (Casillas et al., 2017). According to the calculation using the Debye-Scherrer formula, it was found that the smallest crystal size was obtained by ZnO-Al_2O_3 (1:0.05) with a 13.3 nm crystal size. Therefore, the composite that will be used in the application of Remazol Red RB dye photodegradation is ZnO-Al_2O_3 (1:0.05).

Figure 2 (a) shows that the surface of ZnO had irregular granules with non-uniform size. Furthermore, Figure 2 (b) shows that the surface of ZnO-Al_2O_3 (1:0.05) had granules shaped with a smaller particle size than the constituent particles of ZnO and the shape tends to agglomerate.

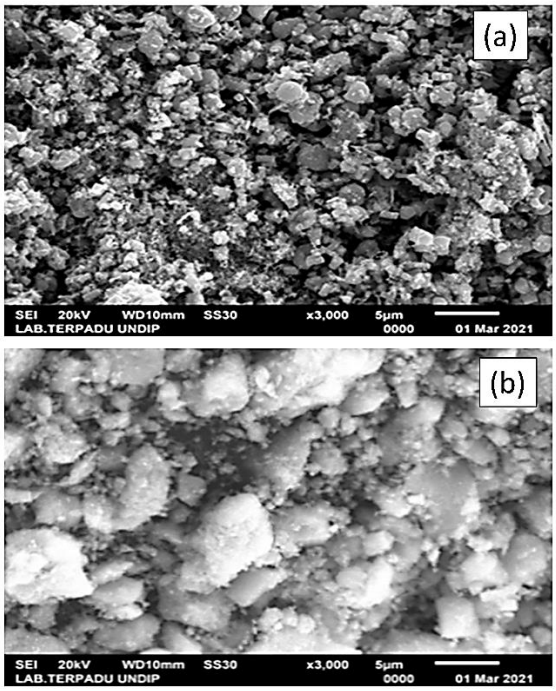

Fig. 2: The morphology surface at 3000x magnification of (a) ZnO and (b) ZnO-Al_2O_3 (1:0.05)

Table 2. The elemental content of ZnO and ZnO-Al_2O_3 (1:0.05)

Elements	ZnO (%)	ZnO-Al_2O_3 (%)	ZnO (g)	ZnO-Al_2O_3 (g)
Zn	70.45	50.16	0.7045	0.5016
O	17.23	21.26	0.1723	0.2126
Al	-	5.28	-	0.0528

The elemental contents of the ZnO-Al_2O_3 composite (1:0.05) are shown in Table 2. According to Table 2, the constituent elements of Zn and O are 70.45% and 17.23%, respectively. The ZnO-Al_2O_3 (1:0.05) composite consisting of the elements Zn, Al, and O were 50.16%, 21.26%, and 5.28%, respectively. These elements indicate that the modification was successfully carried out (Qaderi et al., 2021). Furthermore, the percentage value indicates that ZnO and ZnO-Al_2O_3 (1:0.05) were successfully synthesized but not optimal. This was possible due to the presence of impurities such as carbon.

In general, semiconductor materials have two energy bands, namely the valence and conduction bands, and the distance between them is called the energy band gap. When an electron in the valence band absorbs the appropriate photon energy, the electron becomes excited to the conduction band. Furthermore, this electron transmits a certain amount of energy when it returns to its ground state. The energy transmitted by the material is proportional to the width of the energy band gap (Shenouda et al., 2020). In addition, the UV-Vis DRS characterization for determining the band gap of the photocatalyst is shown in Figure 3.

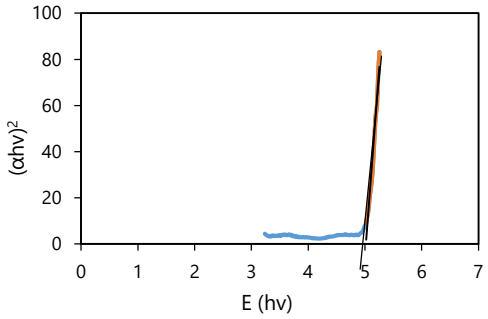

(a)

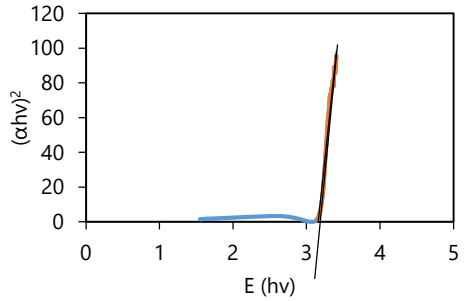

(b)

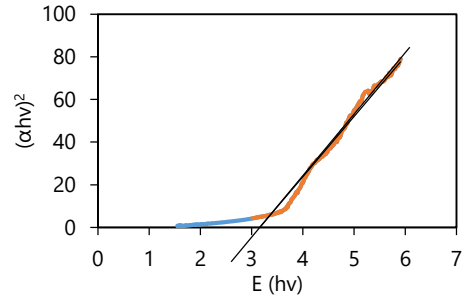

(c)

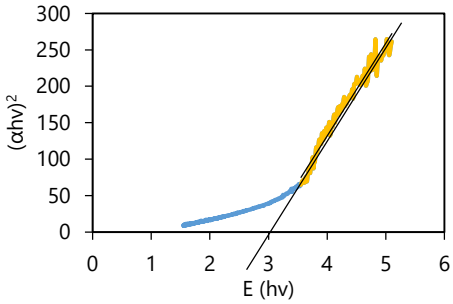

(d)

Fig. 3: UV-Vis DRS curve of (a) ZnO (b) ZnO-Al_2O_3 (1:0.05) (c) ZnO-Al_2O_3 (1:0.07) and (d) ZnO-Al_2O_3 (1:0.10)

Figure 3 (a) shows the energy band gap value of the ZnO composite, which is the result of the intersection of the line between E (hv) on the x-axis, and $(\alpha hv)^2$ on the y-axis and the energy band gap (Eg) was 5.01 eV. Figure 3 (b) shows the energy band gap value of the ZnO-Al_2O_3 composites 1:0.05, 1:0.07, 1:0.10 was 3.16 eV, 3.15 eV, and 2.96 eV, respectively.

ZnO has a band gap energy of 3.37 eV (Benhaoua et al., 2014). Furthermore, the difference between the experimental and literature Eg values is probably due to calcination parameter processes such as temperature and holding time, which correlated with the product characteristics differently (Alibe et al., 2018; Lhimr et al., 2021). Furthermore, the difference between the two increased pure and impure ZnO band gaps was also reported by Akhtar et al. (2015). The shift towards the conduction band was due to the addition of Al charges which resulted in the wide band gap. The curve and calculations show that the energy band gap decreases with increasing Al concentration in the ZnO-Al_2O_3 composite. This condition indicates the success of the synthesis of the Al_2O_3-ZnO composite. Furthermore, the smaller the band gap energy value, the lesser the energy needed by the photocatalyst to excite electrons from the valence to the conduction band. This gives more advantages to photocatalyst applications because it works over a wider range of wavelengths and can be applied to the visible light region (Modwi et al., 2018).

pH Point Zero Charge (pHpzc) ZnO-Al_2O_3 (1:0.05)

pHpzc is the pH value at the surface of an uncharged oxide that is uncharged or in a neutral charge (Ngulube et al., 2017). When pH<pHpzc, the surface of the photocatalyst is positively charged, while at pH>pHpzc is negative (Stjepanović et al., 2021). Furthermore, photocatalysts with positive and negative charged surfaces were able to degrade both anionic and cationic pollutants.

(Elhalil et al., 2018). The pHpzc data is used to determine the appropriate pH state in the photodegradation application process. The pHpzc curve data is shown in Figure 4.

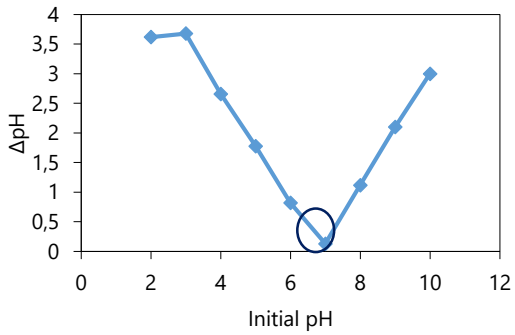

Fig. 4: pHpzc of ZnO-Al_2O_3 (1:0.05)

According to Figure 4, the pHpzc composite ZnO-Al_2O_3 (1:0.05) was at pH 6.87, indicating the presence of ZnO-Al_2O_3.

The dye used in the photodegradation application process was an anionic dye called Remazol Red RB. Therefore, the pH of the solution below pHpzc is favorable. The pH range of this dye which had been measured previously, was pH 5-6.

Photodegradation of Remazol Red RB

Effect of Photodegradation Time

Figure 5 shows the effect of photodegradation time on the removal of Remazol Red RB.

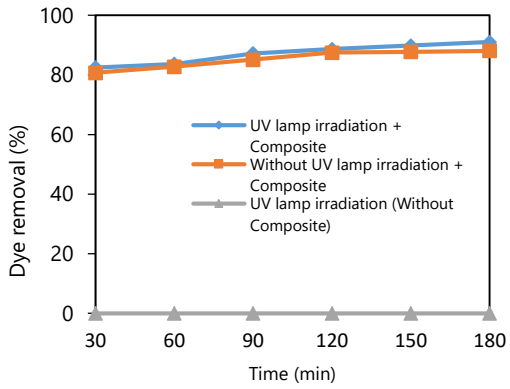

Fig. 5: Effect of photodegradation time on the removal of Remazol Red RB dye concentration reduction

Figure 5 revealed that there was an increase in the removal of Remazol Red RB in the range of 30 to 180 minutes under conditions using UV lamp irradiation from 82.50 to 91.04%. It can be seen that the maximum degradation occurred at 180 minutes with a 91.04% percentage of removal. The increase in the removal of the concentration of Remazol Red RB was relatively constant. A similar trend was reported by a previous study (Alshabanat & Al-Anazy, 2018) using Polymer nanocomposite Films for congo red photodegradation. The removal of photodegradation is positively correlated to the production of OH•. Therefore, the more OH• produced, the more photodegradation occurs (Luo et al., 2017). According to Figure 5, at equilibrium conditions, the ability of the photocatalyst to excite electrons (e-) from the valence to the conduction band may not be increased. Therefore, either the amount of OH• remains constant, or the possibility of OH• produced is used to degrade intermediate products.

Comparative control was also carried out on variations in photodegradation time, such as the treatment of Remazol Red RB dye, which was added to ZnO-Al_2O_3 (1:0.05) without being exposed to a UV lamp (comparative control I) and the Remazol Red RB exposed to UV light without composite (comparative control II). Figure 5 shows that in the comparison control I, there was also an increase in the removal of Remazol Red RB with a longer duration. The dye removal of comparative control I was slightly smaller than that of UV lamp irradiation, which was 88.10%. Furthermore, the longer the irradiation contact time in the reaction system, the larger the amounts of adsorption products formed (Fajriati et al., 2019). However, this may block the contact between

the photocatalyst and UV light and also between the photocatalyst and the dye that has not been degraded. As a result, the photodegradation reaction is not very effective.

There was a difference in the dye removal between the process with UV lamp irradiation and the comparison control I. This is probably because, in the Remazol Red RB dye photodegradation process by ZnO-Al_2O_3 (1:0.05), it undergoes an adsorption process before interacting with UV light. Furthermore, in comparison control II there was no change in the dye removal despite being exposed to the UV lamp. This shows that irradiation with UV lamps, even with varying contact times, without adding ZnO-Al_2O_3 (1:0.05) composite may not properly assist the Remazol Red RB dye degradation.

Based on the data obtained in Figure 5, it was found that there was only a slight difference between the results from the treatment using UV lamp irradiation with added composites and without using it. This indicates that the synthesized ZnO-Al_2O_3 composite had no significant effect with or without UV lamp irradiation. This also means that the composite acts more as an adsorbent than a photocatalyst. Tajizadegan et al. (2015) reported that Al_2O_3 had been used as an adsorbent in dye adsorption, while zinc oxide (ZnO) has generally been used as a photocatalyst in the photocatalytic degradation of dye compounds in the presence of an artificial UV light source. However, with the adsorption method, ZnO was also used as an adsorbent for dye removal.

Effect of Variation in Initial Concentration of Remazol Red RB

Figure 6 shows the effect of the initial dye concentration of Remazol Red RB on the removal of Remazol Red RB.

From Figure 6, it can be seen that there was an increase in dye removal at 10 to 50 ppm with UV lamp irradiation from 62.50 to 89.26%. This is because the higher the concentration, the greater the amount of dye absorbed on the catalyst's surface. Similar to the effect of photodegradation time, comparative control was also carried out.

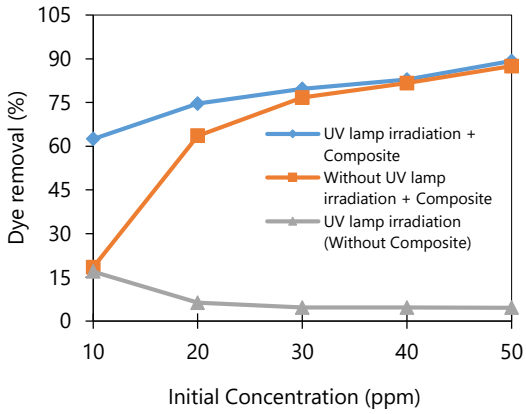

Fig. 6: The effect of initial dye concentration on the removal of Remazol Red RB

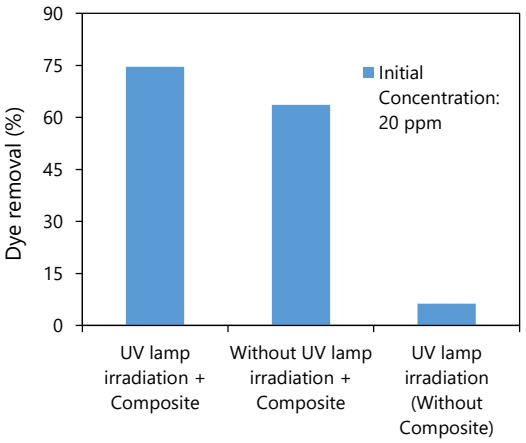

Fig. 7: The effect of irradiation on the removal of Remazol Red RB at the initial concentration of 20 ppm

From comparison control I, it can be seen that there was also an increase in the removal of Remazol Red RB as the initial concentration increased. Furthermore, it rapidly increased from 10 to 20 ppm, while from 30 to 50 ppm, there was only a slight

increase in dye removal. A higher dye concentration indicates more dye molecules; therefore, more photocatalyst is required at a constant intensity of ultraviolet light. Thus, the number of hydroxyl radicals produced by the photocatalyst remains constant. Consequently, the hydroxyl radicals produced were insufficient to oxidize the dyes at higher concentrations (Vu et al., 2020).

The dye removal of comparison control I was smaller when compared to UV lamp irradiation. This was also similar to comparison control II, in which there was a decrease in dye removal. This demonstrates that irradiation with UV lamps without adding ZnO-Al_2O_3 (1:0.05) composite does not optimally promote Remazol Red RB degradation. According to Elhalil et al. (2018), it was reported that Ca-ZnO-Al_2O_3 exhibits more photocatalytic degradation of caffeine than photolysis (UV without photocatalyst). Furthermore, Modwi et al. (2018) also reported that there was no significant photodegradation of malachite green (MG) via photolysis.

CONCLUSIONS

The ZnO-Al_2O_3 composites with mass ratios 1:0.05, 1:0.07, and 1:0.10 were successfully synthesized. The XRD characterization showed a similarity with the typical peak of the JCPDS card No. 36-1451 at an angle of 2θ around 31°. The UV-Vis DRS characterization for the ZnO-Al_2O_3 composite (1:0.05) showed an energy band gap of 3.16 eV. In addition, the surface morphology of the ZnO-Al_2O_3 (1:0.05) composite on the SEM characterization revealed that the surface formed a granule with a smaller particle size than the ZnO constituent. The EDX analysis of ZnO-Al_2O_3 revealed the presence of Zn, Al, and O elements by 50.16%, 21.26%, and 5.28%, respectively. The optimum conditions for dye removal of Remazol Red RB dye in this study were at a contact time of 180 minutes as well as an initial concentration of 50 ppm, with the dye removal of each variable being 91.04% and 89.26%.

ACKNOWLEDGEMENT

The research/publication of this article was funded by DIPA of Public Service Agency of Universitas Sriwijaya 2021. SP DIPA-023.17.2.677515/2021, On November 23, 2020. In accordance with the Rector's Decree Number: 0007/UN9/SK.LP2M.PT/2021, On April 27, 2021.

REFERENCES

Ajala, F., Hamrouni, A., Houas, A., Lachheb, H., Megna, B., Palmisano, L., and Parrino, F. 2018. "The Influence of Al Doping on The Photocatalytic Activity of Nanostructured ZnO: The Role of Adsorbed Water," *Appl. Surf. Sci.*, 445, 376-382.

Akhtar, M. J., Alhadlaq, H. A., Alshamsan, A., Majeed Khan, M. A., and Ahamed, M. 2015. "Aluminum Doping Tunes Band Gap Energy Level as well as Oxidative Stress-Mediated Cytotoxicity of ZnO Nanoparticles in MCF-7 Cells," *Sci. Rep.*, 5, 5.

Alibe, I. M., Matori, K. A., Sidek, H. A. A., Yaakob, Y., Rashid, U., Alibe, A. M., Zaid, M. H. M., and Khiri, M. Z. A. "Effects of calcination holding time on properties of wide band gap willemite semiconductor nanoparticles by the polymer thermal treatment method," *Molecules*, 23(4), 1-18.

Alshabanat, M. N., and Al-Anazy, M. M. 2018. "An Experimental Study of Photocatalytic Degradation of Congo Red Using Polymer Nanocomposite Films," *J. Chem*., 2018.

Benhaoua, B., Rahal, A., and Benramache, S. 2014. "The Structural, Optical and Electrical Properties of Nanocrystalline ZnO:Al Thin Films," *Superlattices Microstruct.*, 68, 2.

Casillas, J. E., Tzompantzi, F., Castellanos, S. G., Mendoza-Damián, G., Pérez-Hernández, R., López-Gaona, A., and Barrera, A. 2017. "Promotion effect of ZnO on the photocatalytic activity of coupled Al_2O_3-Nd_2O_3-ZnO composites prepared by the sol − gel method in the degradation of phenol," *Appl. Catal. B Environ*., 208, 161-170.

Cheshme khavar, A. H., Mahjoub, A., and Bayat Rizi, M. 2017. "Low temperature one-pot synthesis of Cu-doped ZnO/Al_2O_3 composite by a facile rout for rapid methyl orange degradation," *J. Photochem. Photobiol. B Biol*., 175, 37-45.

Elhalil, A., Elmoubarki, R., Farnane, M., Machrouhi, A., Sadiq, M., Mahjoubi F. Z., Qourzal, S., and Barka, N. 2018. "Photocatalytic degradation of caffeine as a model pharmaceutical pollutant on Mg doped ZnO-Al_2O_3 heterostructure," *Environ. Nano-technol. Monit*., 10, 63-72.

Elhalil, A., Elmoubarki, R., Farnane, M., Machrouhi, A., Mahjoubi, F. Z. Sadiq, M., Qourzal, S., and Barka, N. 2018. "Synthesis, characterization and efficient photocatalytic activity of novel Ca/ZnO-Al_2O_3 nanomaterial," *Mater. Today Commun*., 16, 194-203.

Fajriati, N., Mudasir., and Wahyuni, E. T. 2019. "Adsorption and photodegradation of cationic and anionic dyes by TiO2 chitosan nanocomposite," *Indones. J. Chem*., 19(2), 441-453.

Goudarzi, M. and Salavati-Niasari, M. 2018. "Using pomegranate peel powders as a new capping agent for synthesis of CuO/ZnO/Al_2O_3 nanostructures; enhancement of visible light photocatalytic activity," *Int. J. Hydrogen Energy*., 43(31), 14406-14416.

Munawaroh, H., Wahyuningsih, S., and Ramelan, A. H. 2017. "Synthesis and Characterization of Al doped ZnO (AZO) by Sol-gel Method," *IOP Conf. Ser.: Mater. Sci. Eng*., 176, 012049.

Khan, I., Saeed, K., Ali, N., Khan, I., Zhang, B., and Sadiq, M. 2020. "Heterogeneous photodegradation of industrial dyes: An insight to different mechanisms and rate affecting parameters," *J. Environ. Chem. Eng.*, 8(5), 104364.

Lei, C., Pi, M., Xu, D., Jiang, C., & Cheng, B. 2017. "Fabrication of hierarchical porous ZnO-Al_2O_3 microspheres with enhanced adsorption performance," *Appl. Surf. Sci.*, 426, 360–368.

Liu, X., Niu, C., Zhen, X., Wang, J., & Su, X. 2015. "Novel approach for synthesis of boehmite nanostructures and their conversion to aluminum oxide nanostructures for remove Congo red," *J. Colloid Interface Sci.*, 452,116–125.

Lhimr, S., Bouhlassa, S. and Ammary, B. 2021. "Influence of calcination temperature on size, morphology and optical properties of ZnO/C composite synthesized by a colloidal method," *Indones. J. Chem*., 21(3), 537-545.

Luna-Sanguino, G., Tolosana-Moranchel, A., Carbajo, J., Pascual, L., Rey, A., Faraldos, M., and Bahamonde, A. 2020. "Role of surrounding crystallization media in TiO_2 polymorphs coexistence and the effect

on AOPs performance," *Mol. Catal.*, 493, 111059.

Luo, J. L., Wang, S. F., Liu, W., Tian, C. X., Wu, J. W., Zu, X. T., Zhao, W. L., Yuan, X. D., and Xiang, X. 2017. "Influence of different aluminum salts on the photocatalytic properties of Al doped TiO2 nanoparticles towards the degradation of AO7 dye," *Sci. Rep.*, 7(1), 1-16.

M'Arimi, M. M., Mecha, C. A., Kiprop, A. K., and Ramkat, R. 2020. "Recent trends in applications of advanced oxidation processes (AOPs) in bioenergy production: Review," *Renew. Sustain. Energy Rev.*, 121, 109669.

Mcyotto, F., Wei, Q., Macharia, D. K., Huang, M., Shen, C., and Chow, C. W. K. 2021. "Effect of dye structure on color removal efficiency by coagulation," *Chem. Eng. J.*, 405, 126674.

Modwi, A., Ghanem, M. A., Al-Mayouf, A. M., and Houas, A. 2018. "Lowering energy band gap and enhancing photocatalytic properties of Cu/ZnO composite decorated by transition metals," *J. Mol. Struct.*, 1173, 1-6.

Moradipour, P., Dabirian, F., and Moradipour, M. 2020. "Ternary ZnO/$ZnAl_2O_4$/Al_2O_3 composite nanofiber as photocatalyst for conversion of CO_2 and CH_4," *Ceram. Int.*, 46(5), 5566-5574.

Murali, M., Suganthi, P., Athif, P., Sadiq Bukhari, A., Syed Mohamed, H. E., Basu, H., and Singhal, R. K. 2017. "Histological Alterations in The Hepatic Tissues of Al_2O_3 Nanoparticles Exposed Freshwater Fish Oreochromis Mossambicus," *J. Trace Elem. Med. Biol.*, 44, 17.

Nasr, M., Viter, R., Eid, C., Habchi, R., Miele, P., and Bechelany, M. 2018. "Optical and structural properties of Al_2O_3 doped ZnO nanotubes prepared by ALD and their photocatalytic," *Surf. Coatings. Technol.*, 343, 24-29.

Ngulube, T., Gumbo, J. R., Masindi, V., and Maity, A. 2017. "An update on synthetic dyes adsorption onto clay based minerals: A state-of-art review," *J. Environ. Manage.*, 191, 35-537.

Pradhan, P., Alonso, J. C., and Bizarro, M. 2012. "Photocatalytic performance of ZnO: Al films under different light sources," *Int. J. Photoenergy*.

Qaderi, J., Mamat, C. R., and Jalil, A. A. 2021. "Preparation and Characterization of Copper, Iron, and Nickel Doped Titanium Dioxide Photocatalysts for Decolorization of Methylene Blue," *Sains Malays.*, 50(1), 135-149.

Sa-nguanprang, S., Phuruangrat, A., Thongtem, T., and Thongtem, S. 2019. "Preparation of Visible-Light-Driven Al-Doped ZnO nanoparticles Used for Photodegradation of Methylene Blue," *J. Electron. Mater.*, 49(3), 1841-1848.

Saksono, N., Putri, D. A., and Suminar, D. R. 2017. "Degradation of Remazol Red in batik dye waste water by contact glow discharge electrolysis method using NaOH and NaCl electrolytes," *AIP Conf Proc.*, 1823, 3-8.

Sangeeta, M., Karthik, K. V., Ravishankar, R., Anantharaju, K. S., Nagabhushana, H., Jeetendra, K. Vidya, Y. S., and Renuka, L. 2017. "Synthesis of ZnO, MgO and ZnO/MgO by Solution Combustion Method: Characterization and Photocatalytic Studies," *Mater. Today Proc.*, 4(11), 11791-11798.

Shenouda, S. S., Hussien, M. S. A., Parditka, B., Csík, A., Takats, V., and Erdélyi, Z. 2020. "Novel amorphous Al-rich Al_2O_3 ultra-thin films as active photocatalysts for water treatment from some textile dyes," *Ceram. Int.*, 46(6), 7922-7929.

Shu, J., Wang, Z., Huang, Y., Huang, N., Ren, C., and Zhang, W. S. 2015. "Adsorption Removal of Congo Red from Aqueous Solution by Polyhedral Cu_2O Nanoparticles: Kinetics, Isotherms, Thermodynamics and Mechanism Analysis," *J. Alloys Compd*., 633, 339.

Stjepanović, M., Velić, N., Galić, A., Kosović, I., Jakovljević, T., and Habuda-Stanić, M. 2021. "From waste to biosorbent: Removal of congo red from water by waste wood biomass," *Water*., 13(3), 279.

Stojadinović, S., Tadić, N., Radić, N., Stojadinović, B., Grbić, B., and Vasilić, R. 2015. "Synthesis and characterization of Al_2O_3/ZnO coatings formed by plasma electrolytic oxidation," *Surf. Coatings Technol.*, 276, 573-579.

Stojadinović, Stevan, Radić, N., Tadić, N., Vasilić, R., and Grbić, B. 2020. "Enhanced ultraviolet light driven photocatalytic activity of ZnO particles incorporated by plasma electrolytic oxidation into Al_2O_3 coatings co-doped with Ce^{3+}," *Opt. Mater*., 101, 109768.

Tajizadegan, H., Torabi, O., Heidary, A., Golabgir, M. H., and Jamshidi, A. 2015. "Study of methyl orange adsorption properties on ZnO–Al_2O_3 nanocomposite adsorbent particles," *Desalin. Water Treat*., 57(26), 12324-12334.

Tejada-Tovar, C., Villabona-Ortíz, Á., and Gonzalez-Delgado, Á. 2021. "Adsorption of Azo-Anionic Dyes in a Solution Using Modified Coconut (Cocos nucifera) Mesocarp: Kinetic and Equilibrium Study," *Water*, 13(10), 1382.

Vu, A. T., Pham, T. A. T., Tran, T. T., Nguyen, X. T., Tran, T. Q., Tran, Q. T., Tran, Q. T., Nguyen, T. N., Van, D. T., Vi, T. D., Nguyen, C. L. 2020. "Synthesis of nano-flakes Ag·ZnO·activated carbon composite from rice husk as a photocatalyst under solar light," *Bull. Chem. React. Eng. Catal*., 15(1), 264-279.

Zhang, X., Chen, Y., Zhang, S., Q. C. 2017. "High photocatalytic performance of high concentration Al-doped ZnO nano-particles," *Sep. Purif. Technol*., 172, 236-241.